

Electronic Structure of Semiconductor Nanocrystals *

Li Jingbo^{1,†}, Wang Linwang², and Wei Suhui¹

(1 National Renewable Energy Laboratory, Golden, CO 80401, USA)

(2 Lawrence Berkeley National Laboratory, Berkeley, CA 94720, USA)

Abstract : This paper reviews our recent development of the use of the large-scale pseudopotential method to calculate the electronic structure of semiconductor nanocrystals, such as quantum dots and wires, which often contain tens of thousands of atoms. The calculated size-dependent exciton energies and absorption spectra of quantum dots and wires are in good agreement with experiments. We show that the electronic structure of a nanocrystal can be tuned not only by its size, but also by its shape. Finally, we show that defect properties in quantum dots can be significantly different from those in bulk semiconductors.

Key words : electronic structure; semiconductor; nanocrystals

EEACC : 2520

CLC number : TN304

Document code : A

Article ID : 0253-4177(2006)02-0191-06

1 Introduction

During the last decade, semiconductor nanocrystals such as quantum dots (QDs) and quantum wires (QWs)^[1] have attracted much attention because the physical properties of the nanocrystals such as the band gap and optical transitions can be tailored continuously by size or shape. This feature opens up great potential for novel device applications from lasers to solar cells to single-electron transistors^[2-4]. Many of these applications require knowledge of the size- and shape-dependence of the nanocrystal's optical properties, which, in a semiconductor, are related to the transitions near the electronic bandgaps. Therefore, studying the size- and shape-dependence of the electron bandgaps and the related exciton energies is one of the most important topics in semiconductor nanocrystal research.

Nanocrystals can be grown in various media, such as polymers, cavities of zeolites, glasses, solutions, and organic molecules or biomolecules^[5]. In many cases, the surface dangling-bond states of the nanocrystal are removed by the medium through passivation. In these cases, the electronic and optical properties of the nanocrystal are the

intrinsic properties of the nanosystem, independent of the enclosure medium and surface passivation. Therefore, one of the important topics in nanostructure study is to understand these intrinsic properties of nanocrystals.

Most of the previous studies focused on the size dependence of physical properties of QDs. Recent developments in chemical synthesis^[6] show that, in addition to the size, the shape of a nanocrystal can also be controlled during growth. It has also been shown recently^[6] that changes in shape can lead to drastically different electronic states and energy bandgaps in nanocrystals. For example, by changing the shape, it is possible to change the location of the holes and electrons; therefore, there is either an increase or decrease in the recombination rate, which is very useful in light-emission applications.

The application of semiconductor nanocrystals as novel electronic devices also depends critically on doping properties. Most semiconductors are not very useful if insufficient charge carriers are generated by the dopants at normal working temperatures. Defect properties have been extensively studied in the past for bulk semiconductors, and various approaches have been proposed to overcome the doping limit in semiconductors^[7].

* Project supported by the U. S. DOE (Nos. DE-AC36-99GO10337 and DE-AC03-76SF0098)

† Corresponding author. Email: Jingbo_Li @nrel. gov

However, very few studies have been carried out to understand how the formation of QDs affects the defect properties in these systems. For example, it is not clear how the size of QDs affects the defect formation energies and ionization energy levels, as well as the relative stability between different defects.

In this paper, we describe our recent developments in the theoretical study of the electronic structure of semiconductor nanocrystals by large-scale numerical calculations^[8-19].

2 Method of calculations

Several methods have been used in our study of the electronic structure of nanocrystals. The first method is the first-principles band-structure method within the density functional theory (DFT) as implemented in pseudopotential codes such as VASP^[20] and PEtot^[21]. This is the most accurate approach and is used as a benchmark to test all other approaches. However, despite the recent rapid growth of computing power, systems that can be handled using this approach are still limited to a few hundred atoms per cell. It also suffers, in some cases, from the bandgap error associated with the DFT method. To overcome this disadvantage, in the last few years, we have developed several new approaches that can give approximate but reliable results on the electronic structure of nanocrystals. One of the approaches is the semi-empirical pseudopotential method (SEPM). In the SEPM approach, the electron wave functions are expanded by plane-wave basis functions as in the *ab initio* pseudopotential methods. The screened SEPM atomic potentials are fitted to the DFT potentials and experimental band structures and are tested extensively for transferability and reliability. Using the SEPM pseudopotential, the single particle's Schrödinger equation is solved non-self-consistently using the linear scaling folded spectrum method^[19] for several states near the bandgap. This approach solves two problems simultaneously: the bandgap error in the DFT and the inability to solve large systems using the current self-consistent DFT method. With modern large-scale supercomputers, this method can be used to calculate systems containing tens of thousands of atoms.

Although quite successful, the SEPM approach suffers from the difficulty in finding a suitable surface-passivation potential because the potentials are usually fitted to bulk semiconductor properties. To overcome this difficulty, we have developed the "charge patching method" (CPM)^[21], which has the accuracy of first-principles DFT, while also handling large systems. In the CPM method, we first generate the *ab initio* quality electron charge density $\rho_{\text{patch}}(\mathbf{r})$ using charge motifs generated from prototype systems with similar atomic environments. After that, the total local-density-approximation (LDA) potential $V(\mathbf{r})$ is obtained by solving Poisson's equation and the standard LDA formula. The single-particle Schrödinger equation can then be solved using the linear scaling folded spectrum method for the band edge states. The surface of the nanocrystal is passivated by a pseudo-hydrogen atom (e.g., 1.25-charge H to passivate the surface Ga-atom dangling bonds, and 0.75-charge H to passivate the surface As-atom dangling bonds in GaAs QDs). Furthermore, to describe the quantum confinement effects accurately, we correct the effective-mass, which is also underestimated in DFT. This method is denoted by "LDA + C". The details of this entire procedure are published in Ref. [18].

3 Size dependence of exciton energies and absorption spectra

We have systematically calculated the exciton transition energy and optical absorption spectrum of QDs and QWs from group III-V (GaAs, InAs, InP, GaN, AlN, and InN) and group II-VI (CdSe, CdS, CdTe, ZnSe, ZnS, ZnTe, and ZnO)^[18] as a function of diameter. The electron-hole Coulomb binding energies are included in these calculations.

Our calculated results are generally in good agreement with experimental measurements. Figure 1 compares our calculated results with the experimental exciton transition energy for CdSe QWs. Our calculations are performed using both the SEPM and LDA + C approaches. We find that the two theoretical results agree well with each other and with experiment. The results can be fitted to the form $E_g = \gamma/d$, where γ is close to 1.3, which is significantly smaller than the simple ef-

fective-mass value of 2 (see below).

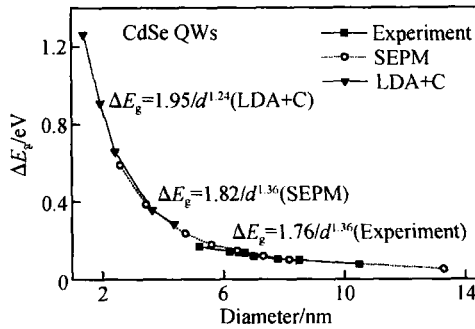


Fig. 1 Comparison of the quantum confinement energy gap of CdSe QWs among experiment, LDA + C, and SEPM calculations

Figure 2 shows the calculated absorption spectrum for CdS QDs with different sizes and the assigned peaks. These spectra are characterized by a large gap between the lower peaks (a, b) and higher peaks (c, d, e, f). This calculated result invites experimental confirmation.

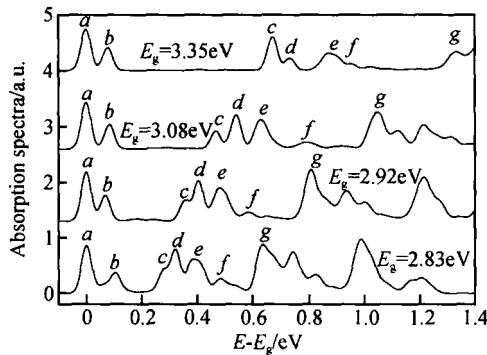


Fig. 2 Calculated optical absorption spectra of CdS QDs with different sizes. The Coulomb interaction is taken into account in the calculation. E_g is the ground exciton energy.

4 Effects of shape on electronic states of nanocrystals

We have studied how the shape of a nanocrystal can be used to engineer the electronic states and its effect on device design. By analyzing our results for CdSe nanosystems^[10], we have compiled the following simple rules that can be used to predict the effects of shape on the electronic structures in similar nanosystems: (1) The atomic character of the hole wavefunction can be predominantly either $p_{x,y}$ or p_z , or have mixed character. The $p_{x,y}$ character tends to be located

at the wider part of the shape, and the p_z character tends to be located at the elongated part of the shape. (2) There is no one-to-one correspondence between the overall shapes of the electron and the hole states. In the wide shapes, the higher electron states tend to develop nodes along the c -axis, whereas the hole states tend to develop nodes in the x, y plane. (3) It is the overall shape that controls the qualitative pictures of the single-particle states. When there is asymmetry, the higher electronic states tend to occupy the smaller end of the shape, whereas the hole states tend to avoid it. (4) The first electron state is highly localized in the central region of a tetrapod. This is mainly because the electron prefers to stay in the zinc-blend (ZB) region, whereas the hole prefers to stay in the wurtzite (WZ) region due to the WZ/ ZB band alignment.

Figures 3 (a) and (b) show branched tetrapods with CdSe central tetrapods and terminal CdTe branches. This material is interesting because of its unusual charge-separating properties. The sharp reduction in spatial overlap between the electrons and holes, apparent in Figs. 3(a) and (b), effectively quenches the bandgap photolumi-

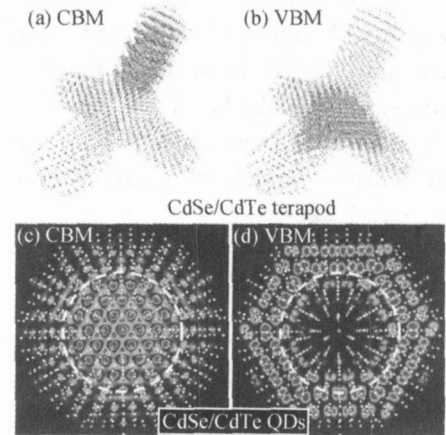


Fig. 3 Wavefunction charge distribution of (a) conduction band minimum (CBM) and (b) valence band maximum (VBM) states for CdSe/ CdTe branched tetrapod, (c) CBM and (d) VBM states for CdSe/ CdTe core/shell structured QDs

nescence^[8]. Other effects, such as the band alignment and strain can also change the charge distribution of holes and electrons^[13]. Figures 3(c) and (d) show the core/shell structure of CdSe/ CdTe QDs, indicating that in this system, the electron state is localized within the core, whereas the hole

state is localized within the shell.

5 Ratios of bandgap increases between QWs and QDs

According to an overly simplified particle-in-a-box effective-mass model^[22,23], the bandgap increases of QDs and QWs from the bulk value are given by $E_g = \frac{2\hbar^2}{m^*d^2}$, where $\frac{1}{m^*} = \frac{1}{m_e^*} + \frac{1}{m_h^*}$ (m_e^* and m_h^* are the electron and hole effective-masses, respectively), and d is the diameter. For spherical QDs, $\alpha = 2.048$ is the zero point of the spherical Bessel function, whereas for cylindrical QWs, $\alpha = 2.4048$ is the zero point of the cylindrical Bessel function. Thus, the ratio of the bandgap increase between QWs and QDs should be $E_g^{\text{wire}}/E_g^{\text{dot}} = 0.586$.

We have systematically studied the electronic structures of surface-passivated QDs and QWs for a wide variety of II-VI and III-V semiconductor compounds^[10]. We find that both the calculated QW and QD bandgaps can be fitted well by the formula $E_g = \alpha^2/d$ with material-dependent parameters α and β . We find that for a given material, QWs and QDs have the same $1/d$ scaling, and the ratios of QW and QD band gap changes are very close to 0.586 for most direct bandgap materials. However, the calculated values^[12] are significantly different from 2, which are obtained from the simple particle-in-a-box effective-mass model.

6 Defect properties in QDs

We have also studied the effects of QD size on the stability and transition energy levels of defects in semiconductors^[19]. The defect formation energy and defect transition-energy levels are calculated using the supercell approach, where a defect is put at the center of a large supercell and periodic boundary conditions are applied. All the internal structural parameters are relaxed by minimizing the quantum mechanical force and total energy until the change in the total energy is less than 0.1 meV/atom.

Figure 4 (a) shows the formation energy of neutral Si_{Ga}^0 in GaAs QDs as a function of the diameter of the dots. The diameter $d = \infty$ corresponds to the bulk system. As the size of the QDs

decreases, the formation energy of Si_{Ga}^0 increases from 1.55eV for bulk GaAs:Si to 2.99eV for a QD with $d = 1.55\text{nm}$. This increase is because Si_{Ga}^0 creates a singly occupied level near the CBM. This level has a strong CBM's character and moves up in energy with the CBM as the QD size decreases, thus increasing the formation energy. However, because this defect level is not a pure CBM state, as the CBM moves up in energy with the decrease of QD size, the energy differences between the defect level and the CBM, and thus the $(0/+)$ transition energy level from the CBM, also increase. The calculated transition energy levels as a function of QD size are shown in Fig. 4 (b). We find that the calculated $(0/+)$ level of Si_{Ga} is very shallow at 6meV below the CBM in the bulk system, in good agreement with experimental results. It increases to 162meV for the smallest QD studied in this work. These results indicate that n-type doping using Si as a dopant will be much more difficult in small QDs than in bulk GaAs.

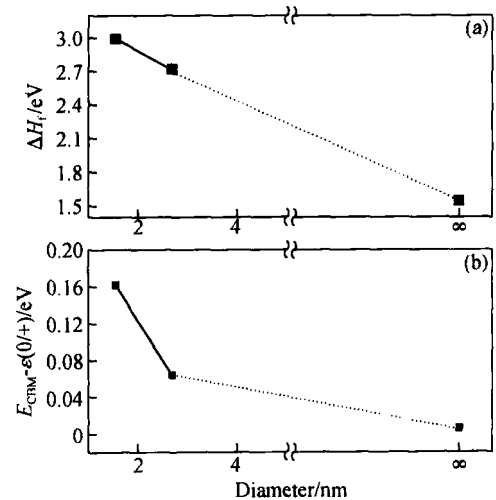


Fig. 4 Formation energy of neutral Si_{Ga}^0 in Si-doped GaAs (a) and transition energy $(0/+)$ (referenced to CBM) of Si_{Ga} in GaAs QDs (referenced to VBM) (b) as a function of diameter

We have also studied the relative stability of the DX center in GaAs Si QDs^[19]. The DX formation energy is defined as the energy difference:

$E(\text{DX}) = E(\text{DX}^-) - E(\text{Si}_{\text{Ga}}^-)$, where $E(\text{DX}^-)$ is the total energy of the negatively charged DX center and $E(\text{Si}_{\text{Ga}}^-)$ is the total energy of the corresponding tetrahedral-coordinated defect Si_{Ga} at the same charge state. A negative $E(\text{DX})$ will

indicate that the DX center is more stable than Si sitting at the substitutional Ga site. The calculated results are shown in Fig. 5. In bulk GaAs, the Si-doped DX formation energy is positive, indicating that the formation of the DX center is not favored in bulk GaAs Si. However, as the size of the QDs decreases and the corresponding bandgap E_g increases, the DX formation energy becomes less positive and changes sign when the bandgap is close to $E_g = 1.78\text{eV}$, which is about 0.26eV larger than the experimental bandgap. We have previously shown^[12] that the bandgap increases of GaAs QDs due to quantum confinement can be expressed as $E_g = 3.88/d^{1.01}$. Using this expression, we therefore estimate that the Si DX center in GaAs will become stable when the diameter of the QD is less than 14.5nm .

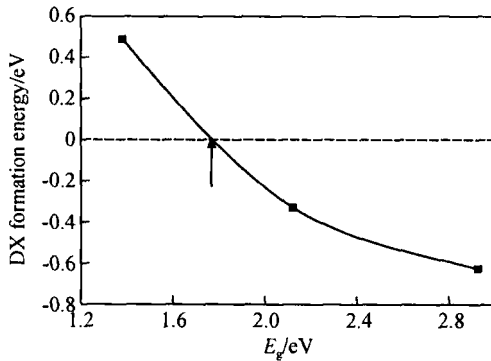


Fig. 5 DX formation energy as a function of the calculated bandgap of GaAs QDs. Arrow indicates the bandgap $E_g = 1.78\text{eV}$, at which the DX⁻ is stabilized. The corresponding QD diameter d is about 14.5nm .

The origin of the enhanced stability of the DX center due to the quantum confinement can be understood as follows: The quantum confinement increases the CBM energy. For the negatively charged Si_{Ga}^- at the T_d site, the shallow defect level has mostly the CBM s wavefunction character. Thus, the energy level of Si_{Ga}^- is expected to follow the CBM closely. But for the DX center, the Si impurity undergoes a large Jahn-Teller distortion along the $\langle 111 \rangle$ direction. Consequently, the level repulsion between the a_1 (a_{1c}) with a_1 (t_{2c}) states mixes a significant amount of atomic p orbital into the wavefunction, so the DX⁻ level does not follow the CBM closely. Therefore, in QDs, when the bandgap increases, the energy difference between the occupied DX⁻ and Si_{Ga}^- levels also increases, thus stabilizing the DX cen-

ter.

7 Summary

In summary, we have described salient features of the electronic structures of semiconductor nanocrystals calculated using our recently developed large-scale pseudopotential method. The calculated size-dependent exciton energies and absorption spectra of quantum dots and wires agree well with experiments. We show that the electronic structure of a nanocrystal not only can be tuned by its size, but also by its shape. Finally, we show that defect properties in quantum dots can be significantly different from those in bulk semiconductors.

Acknowledgment The use of computer resources of the NERSC is greatly appreciated.

References

- [1] Alivisatos A P. Semiconductor clusters, nanocrystals, and quantum dots. *Science*, 1996, 271 :933
- [2] Achermann M, Petruska M A, Kos S, et al. Energy-transfer pumping of semiconductor nanocrystals using an epitaxial quantum well. *Nature*, 2004, 429 :642
- [3] Huynh W U, Dittmer J J, Alivisatos A P, et al. Hybrid nanorod-polymer solar cell. *Science*, 2002, 295 :2425
- [4] Klein D L, Roth R, Lim A K, et al. A single-electron transistor made from a CdSe nanocrystal. *Nature*, 1997, 389 :699
- [5] Woggon U. Optical properties of semiconductor quantum dots. Berlin :Springer-Verlag, 1996
- [6] Manna L, Scher E C, Alivisatos A P. Synthesis of soluble and processable rod-, arrow-, teardrop-, and tetrapod-shaped CdSe nanocrystals. *J Am Chem Soc*, 2000, 122 :12700
- [7] Wei S H. Overcoming the doping bottleneck in semiconductors. *Comp Mater Sci*, 2004, 30 :337
- [8] Milliron D, Hughes S M, Cui Y, et al. Colloidal nanocrystal heterostructures with linear and branched topology. *Nature*, 2004, 430 :190
- [9] Li J, Wang L W. High energy excitations in CdSe quantum rods. *Nano Lett*, 2003, 3 :101
- [10] Li J, Wang L W. Shape effects on electronic states of nanocrystals. *Nano Lett*, 2003, 3 :1357
- [11] Li J, Wang L W. Electronic structure of InP quantum rods : differences between wurtzite, zinc-blende, and different orientations. *Nano Lett*, 2004, 4 :29
- [12] Li J, Wang L W. Comparison between quantum confinement effects of quantum wires and dots. *Chem Mater*, 2004, 16 :4012
- [13] Li J, Wang L W. First principle study of core/shell structure quantum dots. *Appl Phys Lett*, 2004, 84 :3648
- [14] Li J, Wang L W. Deformation potentials of CdSe quantum dots. *Appl Phys Lett*, 2004, 85 :2929
- [15] Wang L W, Li J. First-principles thousand-atom quantum dot

- calculations. *Phys Rev B*, 2004, 69:153302
- [16] Yu H, Li J, Loomis R A, et al. Two-versus three-dimensional quantum confinement in InP wires and dots. *Nature Mater*, 2003, 2:517
- [17] Yu H, Li J, Loomis R A, et al. CdSe quantum wires and the transition from 3D to 2D confinement. *J Am Chem Soc*, 2003, 125:16168
- [18] Li J, Wang L W. Band-structure-corrected local density approximation study of semiconductor quantum dots and wires. *Phys Rev B*, 2005, 72:125325
- [19] Li J, Wei S H, Wang L W. Stability of DX center in GaAs quantum dots. *Phys Rev Lett*, 2005, 94:185501
- [20] Kresse G, Hafner J. Ab initio molecular dynamics for liquid metals. *Phys Rev B*, 1993, 47:558
- [21] Wang L W. Charge-density patching method for unconventional semiconductor binary systems. *Phys Rev Lett*, 2002, 88:256402
- [22] Xia J B, Li J. Electronic structure of quantum spheres with wurtzite structure. *Phys Rev B*, 1999, 60:11540
- [23] Li J, Xia J B. Exciton states and optical spectra in CdSe nanocrystallite quantum dots. *Phys Rev B*, 2000, 61:15880

